Electric Power Components and Systems, 00(00):1–13, 2015

ISSN: 1532-5008 print / 1532-5016 online
DOI: 10.1080/15325008.2015.1061620

Taylor & Francis
Taylor & Francis Group

Optimal Power Flow Using a Hybrid Optimization Algorithm of Particle Swarm Optimization and Gravitational Search Algorithm

Jordan Radosavljević, Dardan Klimenta, Miroljub Jevtić, and Nebojša Arsić
Faculty of Technical Sciences, University of Priština in Kosovska Mitrovica, Kosovska Mitrovica, Serbia

CONTENTS

Abstract—This article presents a hybrid algorithm based on the particle swarm optimization and gravitational search algorithms for solving optimal power flow in power systems. The proposed optimization technique takes advantages of both particle swarm optimization and gravitational search algorithms by combining the ability for social thinking in particle swarm optimization with the local search capability of the gravitational search algorithm. Performance of this approach for the optimal power flow problem is studied and evaluated on standard IEEE 30-bus and IEEE 118-bus test systems with different objectives that reflect fuel cost minimization, voltage profile improvement, voltage stability enhancement, power loss reduction, and fuel cost minimization with consideration of the valve point effect of generation units. Simulation results show that the hybrid particle swarm optimization–gravitational search algorithm provides an effective and robust high-quality solution of the optimal power flow problem.

1. INTRODUCTION

The optimal power flow (OPF) problem has significant importance in a power system's operation, planning, economic scheduling, and security. The OPF problem solution aims to optimize a chosen objective function though optimal adjustment of the power system control variables while simultaneously satisfying various system operations, such as power flow equations and inequality constraints [1]. In its most general formulation, OPF is a non-linear, non-convex, large-scale, static optimization problem with both continuous and discrete control variables.

The OPF problem has been solved by using deterministic (classical) [2] and population-based optimization methods [3]. Classical optimization methods, such as linear programming (LP), non-linear programming (NLP), quadratic programming (QP), Newton (N), sequential quadratic programming (SQP), and interior point method (IPM), are based on an estimation of the global optimum. However, due to difficulties of differentiability, non-linearity, and non-convexity, these methods failed to provide the global optimum and only reached the local one.

Keywords: optimal power flow, particle swarm optimization, gravitational search algorithm, hybrid optimization algorithm
Received 22 June 2014; accepted 30 May 2015
Address correspondence to Jordan Radosavljević, Faculty of Technical Sciences, University of Priština in Kosovska Mitrovica, Kneza Miloša 7 38220, Kosovska Mitrovica, Serbia. E-mail: jordan.radosavljevic@pr.ac.rs

Moreover, these methods exhibit some limitations depending on the type of problem, *e.g.*, when the objective function is not available in algebraic form. It becomes essential to develop optimization methods able to overcome these drawbacks and handle such difficulties [1].

In the past two decades, many population-based methods have been used to solve complex constrained optimization problems. Generally, achieving an optimal or a near-optimal solution for a specific problem will require multiple trials as well as appropriate tuning of associated parameters [4]. A wide variety of population-based techniques, such as differential evolution (DE), the genetic algorithm (GA), the adapted GA (AGA), the enhanced GA (EGA), the real-coded GA (RCGA), simulated annealing (SA), evolutionary programming (EP), improved EP (IEP), tabu search (TS), biogeography-based optimization (BBO), artificial bee colony (ABC), teaching–learning-based optimization (TLBO), particle swarm optimization (PSO), the gravitational search algorithm (GSA), and the krill-herd algorithm (KHA), have been applied in solving OPF problems with different objective functions. A review of many of these optimization techniques applied to solve the OPF problem was given in [3].

In recent years, some hybrid algorithms have been proposed to solve the OPF problem. The combination of several population-based algorithms in a hybrid algorithm allows them to exploit the strength of each algorithm. In [4], the authors investigated the possibility of using a recently emerged evolutionary-based approach as a solution for the OPF problem, which is based on the hybrid modified imperialistic competitive algorithm (MICA) and teaching–learning algorithm (TLA) for optimal settings of OPF control variables. Narimani *et al.* presented a new hybrid algorithm based on the PSO and shuffle frog-leaping algorithms (SFLA) for solving OPF in power systems [5]. Niknam and coworkers proposed a hybrid algorithm based on the SFLA and SA for solving the OPF problem with non-smooth and non-convex generator fuel cost characteristics [6]. In [7], a hybrid algorithm consisting of BBO with an adaptive mutation scheme and the concept of predator–prey optimization technique (adaptive biogeography-based predator–prey optimization [ABPPO]) was proposed for solving the multi-objective OPF problems. A hybrid optimization method that combines a harmony search algorithm and an ant system was proposed in [8] for OPF using a flexible AC transmission system.

This article proposes a hybrid PSO and GSA (PSOGSA) algorithm to solve the OPF problem. This algorithm profits from the abilities of both the PSO and GSA. The performance of the proposed algorithm is tested on an IEEE 30-bus test system with different objectives that reflect fuel cost minimization, loss reduction, and voltage profile improvement. Numerical results obtained by the proposed approach were compared with other optimization results reported in the literature recently.

The rest of the article is organized as follows. In Section 2, the OPF is mathematically formulated. Section 3 explains the standard structure of the PSO, GSA, and hybrid PSOGSA. Section 4 presents the results of the optimization and compares the algorithms used to solve the case studies of OPF problems with IEEE 30-bus and IEEE 118-bus system. Finally, Section 5 outlines the conclusion.

2. PROBLEM FORMULATION

Generally, the OPF problem can be formulated as follows [1]:

$$\min J(\mathbf{x}, \mathbf{u}) \tag{1}$$

$$\text{subjectto } g(\mathbf{x}, \mathbf{u}) = 0, \tag{2}$$

$$h(\mathbf{x}, \mathbf{u}) \leq 0, \tag{3}$$

$$\mathbf{u} \in \mathbf{U}, \tag{4}$$

where J is objective function to be minimized; $\mathbf{x}$ is the vector of dependent variables consisting of slack bus power P_{G1}, load bus voltage V_L, generator reactive power output Q_G, and transmission line loading S_l. Accordingly, vector $\mathbf{x}$ can be expressed as

$$\mathbf{x}^T = [P_{G1}, V_{L1} \cdots V_{LNL}, Q_{G1} \cdots Q_{GNG}, S_{l1} \cdots S_{lNTL}], \tag{5}$$

where NL, NG, and NTL are number of load buses, number of generators, and number of transmission lines, respectively.

$\mathbf{u}$ is the vector of control variables, consisting of generator active power outputs P_G (except at the slack bus P_{G1}), generator voltages V_G, transformer tap settings T, and shunt VAR compensations Q_C. Hence, $\mathbf{u}$ can be expressed as

$$\mathbf{u}^T = [P_{G2} \cdots P_{GNG}, V_{G1} \cdots V_{GNG}, T_1 \cdots T_{NT}, Q_{C1} \cdots Q_{CNC}], \tag{6}$$

where NT and NC are the number of the regulating transformer and VAR compensators, respectively.

The equality constraints in Eq. (2) are the typical non-linear power flow equations:

$$P_{Gi} - P_{Di} - V_i \sum_{j=1}^{NB} V_j \left(G_{ij} \cos \delta_{ij} + B_{ij} \sin \delta_{ij}\right) = 0, \tag{7}$$

$$Q_{Gi} - Q_{Di} - V_i \sum_{j=1}^{NB} V_j \left(G_{ij} \sin \delta_{ij} - B_{ij} \cos \delta_{ij}\right) = 0, \tag{8}$$

where $i = 1, \ldots, NB$; NB is the number of buses, P_D is the load active power, Q_D is the load reactive power, δ_{ij} is voltage angle between buses i and j, and G_{ij} and B_{ij} are the real and

imaginary terms of bus admittance matrix corresponding to the *i*th row and *j*th column, respectively.

The inequality constraints in Eq. (3) are the functional operating constraints, such as load bus voltage magnitude limits, generator reactive power output limits, and branch flow limits:

$$V_{Li}^{\min} \le V_{Li} \le V_{Li}^{\max}, \quad i = 1, \cdots, NL; \tag{9}$$

$$Q_{Gi}^{\min} \le Q_{Gi} \le Q_{Gi}^{\max}, \quad i = 1, \cdots, NG; \tag{10}$$

$$S_{li} \le S_{li}^{\max}, \quad i = 1, \cdots, NTL. \tag{11}$$

The constraints in Eq. (4) define the feasibility region of the problem control variables, such as generator active power output limits, generator bus voltage magnitude limits, transformer tap setting limits, and shunt VAR compensation limits;

$$P_{Gi}^{\min} \le P_{Gi} \le P_{Gi}^{\max}, \quad i = 1, \cdots, NG; \tag{12}$$

$$V_{Gi}^{\min} \le V_{Gi} \le V_{Gi}^{\max}, \quad i = 1, \cdots, NG; \tag{13}$$

$$T_i^{\min} \le T_i \le T_i^{\max}, \quad i = 1, \cdots, NT; \tag{14}$$

$$Q_{Ci}^{\min} \le Q_{Ci} \le Q_{Ci}^{\max}, \quad i = 1, \cdots, NC. \tag{15}$$

It is worth mentioning that the control variables are self-constrained. The inequality constraints of the dependent variables contain P_{G1}, V_L, Q_G, and S_l, added to the objective function as a quadratic penalty terms [9]. The new expanded objective function to be minimized becomes

$$J_p = J + \lambda_P \left(P_{G1} - P_{G1}^{\lim}\right)^2 + \lambda_V \sum_{i=1}^{NL} \left(V_{Li} - V_{Li}^{\lim}\right)^2 + \lambda_Q \sum_{i=1}^{NG} \left(Q_{Gi} - Q_{Gi}^{\lim}\right)^2 + \lambda_S \sum_{i=1}^{NTL} \left(S_{li} - S_{li}^{\lim}\right)^2, \tag{16}$$

where λ_P, λ_V, λ_Q, and λ_S are defined as penalty factors; x^{lim} is the limit value of the dependent variable x and is given as $x^{lim} = x^{\max}$ if $x > x^{\max}$ and $x^{lim} = x^{\min}$ if $x < x^{\min}$.

In this study, the initially specified penalty factors were 10^3 for the slack bus active pover (λ_P), 10^5 for voltage limits (λ_V), 10^4 for generator reactive power limits (λ_Q), and 10^3 for branch-power limits (λ_S).

3. HYBRID PSOGSA

3.1. Overview of PSO Algorithm

PSO is basically developed through simulation of bird flocking in two-dimensional space. It uses a number of particles (candidate solutions) that fly around in the search space to find the best solution. Meanwhile, the particles all look at the best particle (best solution) in their paths. In other words, particles consider their own best solutions as well as the best solution found so far. Each particle tries to modify its position using the following information: the current position, the current velocity, the distance between the current position and *Pbest*, and the distance between the current position and *Gbest* [10, 11].

The basic elements of the PSO technique are briefly stated and defined as follows [12].

Particle ($X(t)$): a candidate solution represented by an n-dimensional vector, where n is the number of control variables. At time (iteration) t, the ith particle $X_i(t)$ can be described as $X_i(t) = \left[x_i^1(t), ..., x_i^k(t), ..., x_i^n(t)\right]$, where x denotes the optimized parameters, and $x_i^k(t)$ is the position of the ith particle with respect to the kth dimension, *i.e.*, the value of the kth control variable in the ith candidate solution.

Population ($pop(t)$): a set of N particles at time (iteration) t, *i.e.*, $pop(t) = [X_1(t), \ldots, X_N(t)]^T$.

Swarm: an apparently disorganized population of moving particles that tend to cluster together while each particle seems to be moving in a random direction.

Particle velocity ($V(t)$): the velocity of the moving particles represented by an n-dimensional vector. At time (iteration) t, the ith particle velocity $V_i(t)$ can be described as $V_i(t) = \left[v_i^1(t), ..., v_i^k(t), ..., v_i^n(t)\right]$, where $v_i^k(t)$ is the velocity component of the ith particle with respect to the kth dimension.

Individual best ($Pbest(t)$): as a particle moves through the search space, it compares its fitness value at the current position to the best fitness value it has ever attained at any time up to the current time. The best position that is associated with the best fitness encountered so far is called the individual best, Pbest(t). For the ith particle, the individual best can be expressed as $Pbest_i(t) = \left[pbest_i^1(t), ..., pbest_i^k(t), ..., pbest_i^n(t)\right]$.

Global best ($Gbest(t)$): the best position among all individual best position achieved so far; hence, global best can be expressed as $Gbest(t) = \left[gbest^1(t), ..., gbest^k(t), ..., gbest^n(t)\right]$.

Stopping criteria: the conditions under which the search process will terminate. In this study, the search will terminate if the number of iterations t reaches the maximum allowable number tmax.

The PSO can be mathematically expressed as follows:

$$v_i^k(t+1) = w(t)\, v_i^k(t) + C_1 r_1 \left(pbest_i^k(t) - x_i^k(t)\right) + C_2 r_2 \left(gbest^k(t) - x_i^k(t)\right), \tag{17}$$

$$x_i^k(t+1) = x_i^k(t) + v_i^k(t+1), \tag{18}$$

where $w(t)$ is a weighting factor, C_1 and C_2 are positive constants, and r_1 and r_2 are uniformly distributed random numbers in [0, 1].

The first term of Eq. (17) provides the exploration ability for PSO. For the initial stages of the search process, a large w to enhance the global exploration is recommended, while for the last stages, the weight factor is reduced for better local exploration. The second term of Eq. (17) represents the cognitive part of PSO where the particle changes its velocity based on its own thinking and memory. The third term represents the social part of PSO where the particle changes its velocity based on the social-psychological adaptation of knowledge.

The PSO starts by randomly placing the particles in a problem space. In each iteration, the velocities of particles are calculated using Eq. (17). After defining the velocities, the positions of particles can be calculated as Eq. (18). The process of changing particle positions will continue until an end criterion is met.

3.2. Overview of GSA

The GSA is a newly stochastic search algorithm developed by Rashedi *et al.* [13]. In the GSA, the search agents are a collection of masses that interact with each other based on Newtonian gravity and the laws of motion. In this algorithm, agents are considered as objects and their performances are measured by their masses. All these objects attract each other by the gravity force, and this force causes a global movement of all objects toward the objects with heavier masses. The position of the mass corresponds to the solution of the problem, and its gravitational and inertial masses are determined using a fitness function. In other words, each mass presents a solution. The algorithm is navigated by properly adjusting the gravitational and inertial masses. By lapse of time, the masses will be attracted by the heaviest mass that represents an optimum solution in the search space.

The GSA could be considered as an isolated system of masses. It is like a small artificial world of masses obeying the Newtonian laws of gravitation and motion. In a system with N agents (masses), the position of the ith agent is defined by

$$X_i = \left[x_i^1, ..., x_i^k, ..., x_i^n\right] \text{ for } i = 1, 2, ..., N, \tag{19}$$

where n is the search space dimension of the problem, *i.e.*, the number of control variables, and x_i^k defines the position of the ith agent in the kth dimension.

After evaluating the current population fitness, the mass of each agent is calculated as follows [13]:

$$M_i(t) = \frac{m_i(t)}{\sum_{j=1}^{N} m_j(t)}, \tag{20}$$

where:

$$m_i(t) = \frac{fit_i(t) - worst(t)}{best(t) - worst(t)}, \tag{21}$$

where $fit_i(t)$ represents the fitness value of agent i at time (iteration) t. $best(t)$ and $worst(t)$ are the best and worst fitness of all agents, respectively, defined as follows (for a minimization problem):

$$best(t) = \min_{j\in\{1,...,N\}} fit_j(t), \tag{22}$$

$$worst(t) = \max_{j\in\{1,...,N\}} fit_j(t). \tag{23}$$

According to the Newton gravitation theory, the total force that acts on the ith agent in the kth dimension at time t is specified as follows:

$$F_i^k(t) = \sum_{j\in Kbest, j\neq i} r_j G(t) \frac{M_j(t) M_i(t)}{R_{i,j}(t) + \varepsilon} \left(x_j^k(t) - x_i^k(t)\right), \tag{24}$$

where r_j is a random number in interval [0, 1], $G(t)$ is gravitational constant at time t, $M_i(t)$ and $M_j(t)$ are masses of agents i and j, ε is a small constant and $R_{ij}(t)$ is the Euclidian distance between the two agents i and j, given by the following equation:

$$R_{ij}(t) = \left\| X_i(t), X_j(t) \right\|_2. \tag{25}$$

Kbest is the set of first K agents with the best fitness value and biggest mass, which is a function of time, initialized to K_0 at the beginning and decreased with time. In such a way, at the beginning, all agents apply the force, and as time passes, *Kbest* is decreased linearly, and at the end, there will be just one agent applying force to the others. By the law of motion, the acceleration of the ith agent at time t in the kth dimension is given by following equation:

$$a_i^k(t) = \frac{F_i^k(t)}{M_i(t)}. \tag{26}$$

The searching strategy on this notion can be defined to find the next velocity and next position of an agent. The next velocity of an agent is defined as a function of its current velocity added to its current acceleration. Hence, the next position and next velocity of an agent can be computed as follows:

$$v_i^k(t+1) = r_i v_i^k(t) + a_i^k(t), \tag{27}$$

$$x_i^k(t+1) = x_i^k(t) + v_i^k(t+1), \tag{28}$$

where r_i is a uniform random variable in the interval [0, 1]. This random number is utilized to give a randomized characteristic to the search; x_i^k represents the position of agent i in dimension k, v_i^k is the velocity, and a_i^k is the acceleration.

It must be pointed out that gravitational constant $G(t)$ is important in determining the performance of the GSA. It is initialized at the beginning and will be reduced with time to control the search accuracy. In other words, the gravitational

constant is a function of the initial value G_0 and time t:

$$G(t) = G_0 \exp\left(-\alpha \frac{t}{t\max}\right), \tag{29}$$

where α is a user-specified constant, t is the current iteration, and $t$max is the maximum iteration number. The parameters of maximum iteration $t$max, population size N, initial gravitational constant G_0, and constant α control the performance of the GSA.

3.3. Hybrid PSOGSA

The basic idea of the PSOGSA is to combine the ability for social thinking (*gbest*) in PSO with the local search capability of the GSA [10, 11]. To combine these algorithms, Eq. (30) is proposed as follows:

$$v_i^k(t+1) = r_1 v_i^k(t) + C_1 r_2 a_i^k(t) + C_2 r_3 \left(gbest^k(t) - x_i^k(t)\right), \quad i = 1, 2, \cdots, N,\ k = 1, 2, \cdots, n, \tag{30}$$

where

$v_i^k(t)$ is the velocity component of the ith agent with respect to the kth dimension at iteration t;
C_1 and C_2 are positive constants;
r_1, r_2, and r_3 are uniformly distributed random numbers in [0, 1];
$a_i^k(t)$ is the acceleration component of the ith agent with respect to the kth dimension at iteration t;
$gbest^k(t)$ is the kth dimension of the best solution so far at iteration t;
N is the size of the population (the number of agents); and
n is the search space dimension of the problem, i.e., the number of control variables.

In each iteration, the positions of agents are updated as follows:

$$x_i^k(t+1) = x_i^k(t) + v_i^k(t+1), \quad i = 1, 2, \cdots, N,\ k = 1, 2, \cdots, n. \tag{31}$$

In the PSOGSA, at first, all agents are randomly initialized. Each agent is considered as a candidate solution. After initialization, the gravitational constant and resultant forces among agents are calculated using Eqs. (29) and (24), respectively. After that, the accelerations of agents are defined as Eq. (26). In each iteration, the best solution so far should be updated. After calculating the accelerations and updating the best solution so far, the velocities of all agents can be calculated using Eq. (30). Finally, the positions of agents are updated by Eq. (31). The process of updating velocities and positions will be stopped by meeting an end criterion.

3.4. PSOGSA Implementation

The proposed hybrid PSOGSA approach has been applied to solve the OPF problem. The control variables of the OPF problem constitute the individual position of several agents that represent a complete solution set. In a system with N agents, the position of the ith agent is defined by

$$X_i = \left[x_i^1, ..., x_i^k, ..., x_i^n\right] \text{ for } i = 1, 2, ..., N \text{ and } n = 2NG - 1 + NT + NC. \tag{32}$$

The elements of agent X_i are generator real power output (except the slack generator), generator bus voltages, tap positions of regulating transformers, and reactive power outputs of shunt VAR compensators. Different steps to solve the OPF problem using the PSOGSA are listed as follows.

Step 1: Search space identification. Initialize PSOGSA parameters, such as N, $t$max, G_0, α, C_1, and C_2.
Step 2: Initialization. Generate random population of N agents. The initial positions of each agent are randomly selected between minimum and maximum values of the control variables.
Step 3: Run the power flow program.
Step 4: Calculate the fitness value for each agent. In this article, different objective functions are considered in different cases.
Step 5: Update $G(t)$ (Eq. (29)), $best(t)$ (Eq. (22)), $worst(t)$ (Eq. (23)), and $M_i(t)$ (Eq. (20)) for $i = 1, 2, \ldots, N$.
Step 6: Calculate the total force in different directions using Eq. (24).
Step 7: Calculate the acceleration of each agent using Eq. (26).
Step 8: Calculate the velocity of all agents using Eq. (30).
Step 9: Update each agent's position using Eq. (31).
Step 10: Repeat Steps 3–9 until the stop criteria is reached, that is, maximum number of iterations $t$max.
Step 11: Return best solution; stop.

4. SIMULATION RESULTS

4.1. IEEE 30-bus Test System

The proposed hybrid PSOGSA has been tested on the standard IEEE 30-bus test system with a total demand of 2.834 p.u. at a 100-MVA base. The system line, bus, and generator data are taken from [9].

The IEEE 30-bus test system has six generators at buses 1, 2, 5, 8, 11, and 13 and four transformers with off-nominal tap ratio at lines 6-9, 6-10, 4-12, and 28-27. The lower and upper limits of the transformer tap settings are 0.9 and 1.1 p.u., respectively. In addition, buses 10, 12, 15, 17, 20, 21, 23, 24, and 29 were selected as shunt VAR compensation buses [12]. The lower and upper limits of the shunt VAR compensations are

0.0 and 0.05 p.u., respectively. The minimum and maximum voltages of all generator buses are considered to be 0.95 and 1.1 p.u., respectively.

The algorithm has been implemented in the MATLAB 2011b computing environment (The MathWorks, Natick, Massachusetts, USA) and run on a 2.20-GHz PC with 3.0 GB RAM. Twenty consecutive test runs have been performed for each case examined. The results shown are the best values obtained over these 20 runs. The different algorithms parameters used for the simulation are adopted as follows: for PSO, C_1 and C_2 are set to 2 and w decreases linearly from 0.9 to 0.4; for the GSA, α is set to 10 and G_0 is set to 100; for the hybrid PSOGSA, C_1 and C_2 are set to 2, α is set to 20, and G_0 is set to 1. The population size (N) and maximum iteration number ($t$max) are set to 50 and 200, respectively, for all case studies.

These values were selected after a number of careful experimentations.

4.1.1. Case 1: Minimization of *F*uel *C*ost

The generator cost characteristics f are defined as quadratic cost function of generator power output P_G. The objective function J is minimization of fuel cost for all generators:

$$J = \sum_{i=1}^{NG} f_i\left(P_{Gi}\right) = \sum_{i=1}^{NG} \left(a_i + b_i P_{Gi} + c_i P_{Gi}^2\right), \qquad (33)$$

where a_i, b_i, and c_i are the cost coefficients of the ith generator. For P_{Gi} (in MW), the cost coefficient a_i is in \$/hr, b_i is in \$/MWh, and c_i is in \$/MW^{2}h.

Most of authors considered the lower and upper voltage limits for the load buses to be 0.95 and 1.05 in p.u. [12, 17–20, 23, 24, 26]. However, in some recent papers [1, 7, 14, 25, 27], the load bus voltage limits are taken as 0.95 and 1.10 p.u. To demonstrate the effectivnes of the PSOGSA and a fair comparison of the obtained optimal solution with those that reported in the literature recently, two different versions of Case 1 have been considered:

Case 1a: The voltages of all load buses have been constrained within the limits of 0.95 and 1.05 p.u.

Case 1b: The voltages of all load buses have been constrained within the limits of 0.95 and 1.10 p.u.

The optimal settings of control variables are given in Table 1. It appears that the total fuel cost is highly reduced in both cases (Cases 1a and 1b) compared to the initial case. The convergence of algorithms for the minimum fuel cost is shown in Figure 1. It is clear that the proposed hybrid PSOGSA can converge to its global best in fewer iterations compared with PSO and GSA.

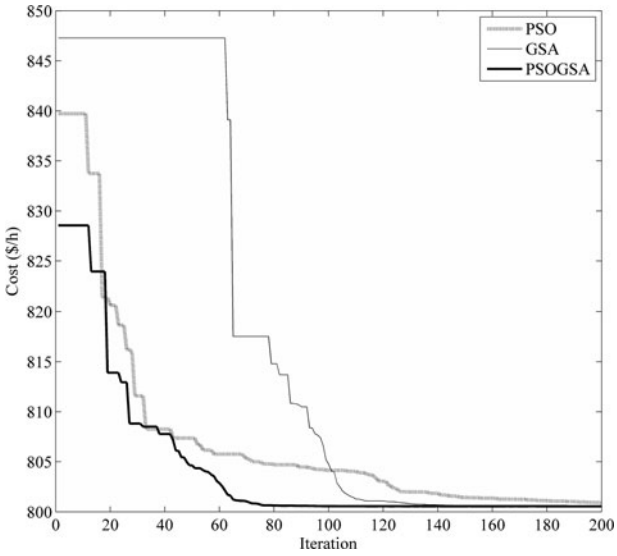

FIGURE 1. Convergence of algorithms for Case 1a.

4.1.2. Case 2: Voltage Profile Improvement

One of the most important and significant safety and service quality indices is bus voltage [14]. Though the minimization of total generation fuel cost may give a feasible solution, the voltage profile may not be acceptable. Therefore, in the present case, a twofold objective function is taken into consideration to minimize the fuel cost and improve voltage profile by minimizing the load bus voltage deviations from 1.0 p.u. The objective function can be expressed as

$$J = \sum_{i=1}^{NG} \left(a_i + b_i P_{Gi} + c_i P_{Gi}^2\right) + w_V \sum_{i=1}^{NL} |V_i - 1.0|, \quad (34)$$

where w_V is a weighting factor for voltage deviation. In this study, the value of w_V is selected as 200. The PSOGSA has been applied to search for the optimal solution of Case 2. These optimal results are given in Table 1. The total fuel cost and voltage deviations are \$804.43123/hr and 0.09638 p.u. for this case compared to \$800.49859/hr and 0.91373 p.u. for Case 1a. Although the cost has been increased by 0.4913%, the voltage deviation has been reduced by 89.45%. The system voltage profile of this case is compared to that of Cases 1a and 1b, as shown in Figure 2. It is evident that the voltage profile is greatly improved compared to that of Case 1a, and especially to Case 1b, which is quite expected considering the upper voltage limits for load buses in this case.

4.1.3. Case 3: Minimization of Fuel Cost and Real Power Loss

In this case, the minimization of the system fuel cost and real power loss are approached. These two competing objectives

	Initial	Case 1a	Case 1b	Case 2	Case 3	Case 4a	Case 4b	Case 5
P_{G1} (MW)	99.22227	177.22184	177.05846	176.17236	127.61738	219.79893	199.56361	177.91887
P_{G2} (MW)	80	48.74698	48.69769	48.42573	51.72966	27.76368	20.00000	49.01737
P_{G5} (MW)	50	21.39255	21.30436	21.60725	29.83039	15.77727	20.81501	21.49628
P_{G8} (MW)	20	21.10061	21.08006	22.60044	34.99994	10.00000	27.94175	22.23327
P_{G11} (MW)	20	11.97192	11.88402	12.61330	24.75936	10.00000	12.84380	10.00000
P_{G13} (MW)	20	12.00006	12.00000	12.00000	19.93146	12.00000	12.06233	12.00000
V_{G1} (p.u.)	1.05	1.08459	1.10000	1.02986	1.10000	1.09264	1.08836	1.06960
V_{G2} (p.u.)	1.04	1.06513	1.08785	1.01837	1.09058	1.06727	1.06504	1.05536
V_{G5} (p.u.)	1.01	1.03370	1.06166	1.01569	1.06752	1.03262	1.03381	1.03487
V_{G8} (p.u.)	1.01	1.03848	1.06940	1.00700	1.07835	1.03505	1.04052	1.04568
V_{G11} (p.u.)	1.05	1.08592	1.10000	1.04449	1.10000	1.10000	1.10000	1.10000
V_{G13} (p.u.)	1.05	1.04114	1.10000	1.00053	1.10000	1.06462	1.06198	1.05126
$T_{11(6\text{-}9)}$ (p.u.)	1.078	1.02559	1.04473	1.06366	1.04293	1.02475	1.03152	1.04235
$T_{12(6\text{-}10)}$ (p.u.)	1.069	0.95857	0.90000	0.90116	0.90000	0.90000	0.90000	0.95619
$T_{15(4\text{-}12)}$ (p.u.)	1.032	0.96478	0.98630	0.95846	0.98097	0.97032	0.96529	0.99467
$T_{36(28\text{-}27)}$ (p.u.)	1.068	0.97458	0.96570	0.96830	0.96771	0.95795	0.96724	0.98518
Q_{C10} (MVAR)	0	3.92906	5.00000	4.67903	5.00000	—	—	4.99995
Q_{C12} (MVAR)	0	3.68477	5.00000	0.00592	5.00000	—	—	5.00000
Q_{C15} (MVAR)	0	4.57095	5.00000	4.98146	5.00000	—	—	5.00000
Q_{C17} (MVAR)	0	5.00000	5.00000	0.00000	4.99999	—	—	4.99965
Q_{C20} (MVAR)	0	4.20562	5.00000	4.99879	5.00000	—	—	5.00000
Q_{C21} (MVAR)	0	5.00000	5.00000	5.00000	5.00000	—	—	5.00000
Q_{C23} (MVAR)	0	3.17397	3.82855	4.99997	3.84156	—	—	5.00000
Q_{C24} (MVAR)	0	5.00000	5.00000	5.00000	5.00000	—	—	5.00000
Q_{C29} (MVAR)	0	2.64020	2.74001	2.58595	2.87091	—	—	4.99994
Cost ($/h)	901.94942	**800.49859**	**799.07055**	**804.43123**	**822.40631**	**824.70959**	**919.65785**	**801.22928**
Ploss (MW)	5.82225	9.03390	8.62457	10.01913	**5.46816**	11.93989	9.82651	9.26567
Voltage deviation (p.u.)	1.14966	0.91373	1.85735	**0.09638**	1.99222	0.73034	0.71741	1.01011
$L_{\max}$	0.17233	0.12674	0.11640	0.13655	0.11513	0.13882	0.13965	**0.12393**

TABLE 1. Optimal solution obtained by PSOGSA for different test cases

Bold indicates the objective function that is optimized.

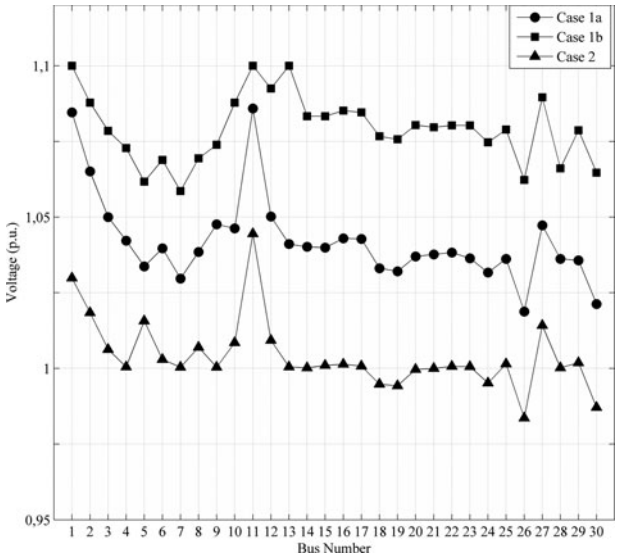

FIGURE 2. System voltage profile.

are optimized simultaneously with the proposed algorithm. The objective function balances the two objectives in such a way that one objective should not dominate the other. The new objective function may be expressed as

$$J = \sum_{i=1}^{NG} \left(a_i + b_i P_{Gi} + c_i P_{Gi}^2\right) + w_{Ploss} Ploss, \qquad (35)$$

where *Ploss* is the total system real power loss and w_{Ploss} is the weighting factor for the real power loss, to be chosen by the user. The value of w_{Ploss} in the present study is selected as 1950. For fair comparison with the results reported in [7, 18], the lower and upper limits of the voltage at load buses was assumed to be 0.95 and 1.10 p.u., respectively.

After applying the proposed algorithm, it appears from Table 1 that the value of power loss is significantly reduced in this case compared to Cases 1b and 2, but the fuel cost and voltage deviation is increased.

4.1.4. Case 4: Minimization of Fuel Cost with Considering the Valve Point Effect.

Large steam turbine generators will have a number of steam admission valves that are opened in sequence to control the power output of the unit. As the unit loading increases, the input to the unit increases and the incremental heat rate decreases between the opening points for any two valves. However, when a valve is first opened, the throttling losses increase rapidly and the incremental heat rate rises suddenly. This is called the valve-point effect, which leads to non-smooth, non-convex input–output characteristics [15]. Usually, the valve-point effect is modeled by adding a recurring rectified sinusoid to the basic quadratic cost function:

$$J = \sum_{i=1}^{NG} a_i + b_i P_{Gi} + c_i P_{Gi}^2 + \left| d_i \sin\left(e_i \left(P_{Gi}^{\min} - P_{Gi}\right)\right)\right|, \tag{36}$$

where d_i and e_i are fuel cost coefficients for valve-point effects; P_{Gi} is in MW, cost coefficient d_i is in p.u., and e_i is in \$/MWh.

For comparison with the reported results, two different cases for the IEEE 30-bus test system have been considered:

Case 4a: minimization of fuel cost considering the valve point effect for all generators. The fuel cost coeficients of the generators are taken from [6, 9].

Case 4b: minimization of fuel cost considering the valve point effect for generators 1 and 2 only. In this case, the fuel cost coefficients of generators 1 and 2 are taken from [16]. The fuel cost coefficients of remaining generators (at buses 5, 8, 11, and 13) have the same values as in Case 4a.

In these cases, the shunt VAR compensators in buses 10, 12, 15, 17, 20, 21, 23, 24, and 29 are ignored, and the voltages at load buses are considered within the range 0.95–1.05 p.u.

The obtained optimal settings of control variables found using the proposed PSOGSA approach are given in Table 1. Figure 3 illustrates the convergence characteristics of the algorithms for Case 4b. As can been seen, the proposed hybrid PSOGSA can converge to its global optima in fewer iterations compared with PSO and GSA.

4.1.5. Case 5: Voltage Stability Enhancement

One important characteristic of the power system is its ability to conserve constantly acceptable bus voltages at each node under normal operating conditions, after load increase, following system configuration changes, or when the system is being subjected to a disturbance. The non-optimized control variables may lead to a progressive and uncontrollable drop in voltage, resulting in an eventual widespread voltage collapse [1, 14].

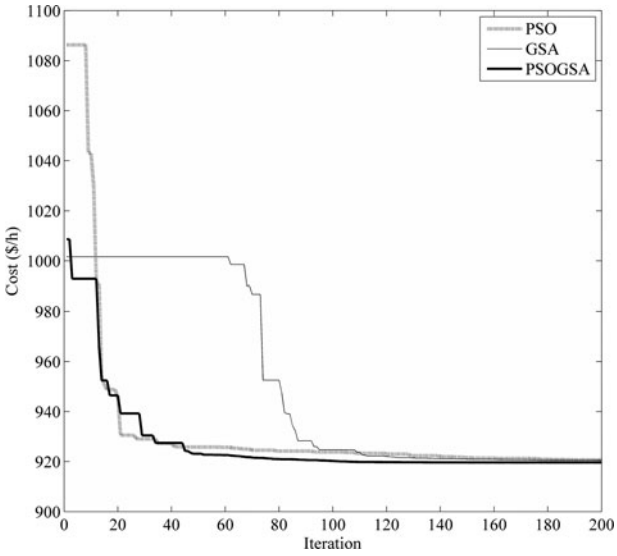

FIGURE 3. Convergence of algorithms for Case 4b.

The static approach for voltage stability analysis involves determination of an index known as a voltage collapse proximity indicator. This index is an approximate measure of closeness of the system operating point to voltage collapse. There are various methods of determining the voltage collapse proximity indicator. One such method is the L-index of the load buses in the system [19].

The L-index gives a scalar number to each load bus. This index uses information on a normal power flow and is in the range of 0 (no-load case) to 1 (voltage collapse). The L-index calculation for a power system was explained in detail in [14, 19, 20, 23, 24]. To enhance the voltage stability and move the system far from the voltage collapse point, the following objective function can be used [1, 12]:

$$J = \sum_{i=1}^{NG} \left(a_i + b_i P_{Gi} + c_i P_{Gi}^2\right) + w_L L_{\max}, \tag{37}$$

where w_L is a weighting factor, and $L_{\max}$ is the maximum value of the L-index, which can be defined as

$$L_{\max} = \max\{L_k\}, \qquad k = 1, \cdots, NL.$$

The vlue of w_L in this case is chosen as 6000. As can be seen from Table 1**,** the minimum fuel cost and index $L_{\max}$ found by the PSOGSA were 801.22928 and 0.12393, respectively; which show a 2.22% reduction in the L-index and about a 0.09% increase in the fuel cost in comparison with Case 1a.

The value of $L_{\max}$ in Case 5 is higher than the values of $L_{\max}$ in Cases 1b and 3, because in those cases, the upper voltage limit at the load buses is considered to be 1.10 p.u.

4.1.6. Comparative Study

Under the same system data, control variable limits, and constraints, the results obtained using the hybrid PSOGSA approach reported herein are compared to some other algorithms reported in the literature, as shown in Table 2. Bold font is used to indicate the proposed algorithm and better performance.

4.1.6.1. Case 1a and Case 1b. For Case 1a, it can be seen in Table 2 that the methods reported in [12, 17, 18, 20, 23] resulted in lesser minimum fuel cost than the proposed PSOGSA approach. However, after the power flow computation with control variables reported in these references, those results can be considered as infeasible solutions. Reasons for infeasibility of those results are sumarized as follows:

- for the best solution given in [12], there were voltage violations at load bus 3;
- for the best solution given in [17], the voltage limits are violated at load buses 3 and 9; the true value of P_{G1} is 178.10537 MW and the total fuel cost is \$800.48421/hr for this violated case;
- the best solution mentioned in [18] is an infeasible solution because there were bus voltage violations at all load buses except at buses 7, 18, 19, 20, 24, 25, 26, 29, and 30;
- for the optimum control variables given in [20], the voltage limits are violated at all load buses;
- for the results reported in [23], the voltage limits are violated at all load buses except at buses 4, 6, 7, and 28; in addition, the reactive power limits of generators at buses 2 and 8 are violated also; the true value of P_{G1} is 177.78284 MW and the exact fuel cost is \$805.43661/hr for this violated case; and
- for the best solution given in [26], the voltage limits are violated at load buses 3, 4, 26, 29, and 30.

The results in Case 1b obtained from the proposed PSOGSA approach were compared to the results reported in [1, 7, 14, 25, 27]. In these works, the load bus voltage limits are assumed to be 0.95 and 1.10 p.u., respectively. Some of those results are marked as incorrect solutions:

- for the optimum control variables given in [7], the true value of P_{G1} is 177.01450 MW, as obtained from the power flow computations, and the total fuel cost for this case is \$799.10122/hr;
- for the optimum control variables given in [14], the true value of P_{G1} is 177.33037 MW, and the total fuel cost for this case is \$799.97946/hr; and
- for the optimum control variables given in [25], the true value of P_{G1} is 177.05766 MW, and the total fuel cost for this case is \$799.08296/hr.

4.1.6.2. Case 2. The results obtained from the proposed PSOGSA was compared to the methods reported in [1, 7, 12, 14, 20, 23, 25, 27]. Some of those results are incorrect solutions, as obtained from the power flow computations:

- for the optimum control variables given in [7], the exact voltage deviation is 0.11302 p.u.;
- for the optimum control variables given in [12], the exact voltage deviation is 0.09622 p.u, and the total fuel cost is \$806.40971/hr;
- for the optimum control variables given in [14], the exact cost is \$804.99389/hr, and the exact voltage deviation is 0.55276 p.u.; and
- for the optimum control variables given in [23], the exact voltage deviation is 0.10700 p.u.

Therefore, it is clear that the OPF result in Case 2 obtained by the PSOGSA is better than those reported in the referenced literature.

4.1.6.3. Case 3. From Table 2, it can be seen that the OPF results in Case 3 obtained by the PSOGSA are either better or comparable to those obtained using methods reported in [7, 18].

4.1.6.4. Case 4a and Case 4b. For Case 4a, the results obtained from the proposed PSOGSA approach was compared to the methods reported in [4, 6, 21]. The best solution given in [4] is an infeasible solution, because the upper voltage limit at bus 3 is violated. From Table 2, it is obvious that the proposed PSOGSA has resulted in less fuel cost than those reported in [4, 6, 21].

The best solution in Case 4b obtained from the proposed PSOGSA approach was compared to the methods reported in [14, 16, 19, 20, 22, 23]. Some of those reported results are incorrect or infeasible solutions:

- for the optimum control variables given in [14], the exact fuel cost is \$962.12485/hr, as obtained from the power flow computations;
- for the optimum control variables given in [16], the lower reactive power limit of the generator at bus 1 is violated; the true value of P_{G1} is 200.66618 MW, and the total fuel cost for this violated case \$926.07046/hr;

Case	Method	Cost ($/h)	*Ploss* (MW)	Voltage deviation (p.u.)	L_{max}
Case 1a	PSO [12]	800.41	—	0.8765	0.1296
	AGA [17]	799.8441	8.9166	0.8043	—
	EGA [18]	799.56	8.697	—	0.111
	ABC [19]	800.66	9.0328	0.9209	0.1381
	BBO [20]	799.1116	8.63	—	—
	GSA [23]	798.6751	8.386	0.87286	0.130759
	EGA [24]	802.06	—	—	—
	GPM [26]	804.853	10.486	—	—
	PSOGSA	**800.49859**	9.03390	0.91373	0.12674
Case 1b	DE [1, 27]	799.2891	8.6150	1.5306	0.1226
	ABPPO [7]	799.0566	8.615	1.8206	0.11796
	TLBO [14]	799.0715	8.6260	1.8925	0.1159
	KHA [25]	799.0311	—	1.9485	0.1265
	PSOGSA	**799.07055**	8.62457	1.85735	0.11640
Case 2	DE [1, 27]	805.2619	10.4412	0.1357	0.1316
	ABPPO [7]	804.7339	10.072	0.09232	0.13648
	PSO [12]	806.38	—	0.0891	0.1392
	TLBO [14]	803.7871	9.8641	0.0945	0.1369
	BBO [20]	804.9982	9.95	0.1020	—
	GSA [23]	804.3148	9.7659	0.093269	0.13578
	KHA [25]	804.6337	—	0.0996	0.1466
	MOMICA[28]	804.9611	9.8212	0.0952	—
	PSOGSA	**804.43123**	10.01913	**0.09638**	0.13655
Case 3	ABPPO [7]	822.7693	5.452	2.05503	0.11546
	EGA [18]	822.87	5.613	—	—
	PSOGSA	**822.40631**	**5.46816**	1.99222	0.11513
Case 4a	MICA-TLA [4]	824.6023	11.9122	—	—
	SFLA-SA [6]	825.6922	—	—	—
	DE [21]	826.54	—	—	—
	RCGA [21]	831.04	—	—	—
	PSOGSA	**824.70959**	11.93989	0.73034	0.13882
Case 4b	TLBO [14]	923.4147	10.9599	1.0282	0.1253
	EP [16]	919.89	—	—	—
	ABC [19]	945.4495	14.0928	0.5284	0.1431
	BBO [20]	919.7647	12.18	—	—
	IEP [22]	953.573	—	—	—
	GSA [23]	929.72405	15.14585	0.577974	0.156484
	PSOGSA	**919.65785**	9.82651	0.71741	0.13965
Case 5	PSO [12]	801.16	—	0.9607	0.1246
	EGA [18]	802.06	—	—	0.1056
	ABC [19]	801.6650	9.2954	0.9380	0.1379
	BBO [20]	805.7252	10.21	—	0.1104
	GSA [23]	806.6013	9.9161	0.9000	0.116247
	PSOGSA	**801.22928**	9.26567	1.01011	**0.12393**

TABLE 2. Comparison of the simulation results

Bold indicates the proposed algorithm and better performance.

- for the optimum control variables given in [20], the true value of P_{G1} is 200.13339 MW, and the total fuel cost for this case is $955.80191/hr; and
- For the optimum control variables given in [23], the reactive power limits of generators at buses 2, 5, and 11 are violated; in addition, the voltages at buses 18, 19, 23, 24, 26, 29, and 30 are less than 0.95 p.u; the true value of P_{G1} is 202.28001 MW, and the exact fuel cost is $945.21117/hr for this violated case.

4.1.6.5. Case 5. The results obtained from the PSOGSA have been compared with other algorithms reported in [12, 18,

	PSO			GSA			PSOGSA		
	Minimum	Maximum	Standard deviation	Minimum	Maximum	Standard deviation	Minimum	Maximum	Standard deviation
Case 1a	800.6199	808.1951	2.1235	800.5356	804.7186	1.1577	800.4981	800.6111	0.0346
Case 1b	799.3586	805.2647	1.9553	799.07123	808.1124	2.0531	799.0705	799.1703	0.0259
Case 2	826.4021	867.7560	10.1548	823.9962	876.4744	10.5366	823.7072	829.6988	1.8387
Case 3	931.2734	958.5769	8.5905	929.6336	966.9396	8.3591	929.0354	930.0418	0.0983
Case 4a	824.8412	830.6802	1.9884	824.7196	837.7094	2.8764	824.7096	824.9921	0.0725
Case 4b	920.6937	946.8402	6.1272	920.6366	955.3907	13.2097	919.6579	924.2865	0.9384
Case 5	1571.0	1619.3	12.2823	1548.9	1590.2	10.9834	1547.2	1552.5	1.6108

TABLE 3. Minimum, maximum, and standard deviation of the results obtained over 20 independent runs with PSO, GSA and PSOGSA

19, 20, 23]. Some of those algorithms have resulted in better performance than the proposed PSOGSA approach. However, it could be shown that those results are indeed infeasible solutions. Reasons for infeasibility of those results are summarized as follows:

- the optimum control variables given in [12] represent an infeasible solution because the reactive powers of the generators at buses 11 and 13 are –10.75 and –15.45 MVAR, respectively; which violate their lower limits;
- the best solution given in [18] is an infeasible solution because reactive powers of the generators at buses 1, 8, 11, and 13 were given as –30.63, 82.61, –12.64, and –17.59 MVAr, respectively; which violate their corresponding limits as reported in [9]; in addition, the bus voltages at all load buses, except bus 30, are higher than their upper limits;
- for the opimum control variables given in [20], the upper limits of the voltages at buses 27 and 29 are violated; and
- the best result given in [23] is an infeasible solution because reactive powers of the generators at buses 8, 11, and 13 are 81.35, –21.63, and –24.45 MVAr, respectively, which violate their limits; in addition, the voltage limits are violated at all load buses.

Based on the comparative study of the simulation results presented in this section, it is can be noted that the proposed PSOGSA approach outperforms many techniques used to solve different OPF problems. This highlights its ability to find better quality solution.

In addition, the comparison of minimum, maximum, and standard deviation of the results obtained by PSO, GSA, and hybrid PSOGSA over 20 runs is presented in Table 3. It is clear that the proposed hybrid PSOGSA approach provides better and more stable solutions compared to the original PSO and GSA.

4.2. IEEE 118-bus Test System

To evaluate the efficiency of the proposed PSOGSA approach in solving a larger power system, the IEEE 118-bus test system is considered. The system data with generator cost coefficients are taken from [29]. The test system has 54 generators, 186 branches, 9 transformers, 2 reactors, and 12 capacitors. It has a total of 129 control variables as follows: 54 generator active powers and bus voltages, 9 transformer tap settings, and 12 shunt capacitor reactive power injections. The voltage limits of all buses are between 0.94 and 1.06 p.u. The transformer tap settings are considered within the interval 0.90–1.10 p.u. The available reactive powers of shunt capacitors are within the range 0–30 MVAR.

One optimization case was considered: the minimization of the total fuel cost of all generators. The objective is as in Case 1 for the IEEE 30-bus test system. The test results obtained using proposed PSOGSA along with PSO and GSA are presented in Table 4. The average CPU time of one iteration for this test system is 6.4 sec. The total fuel cost obtained by the proposed PSOGSA is reduced to be $129,733.58/hr compared to the initial case fuel cost of $131,220.52/hr. The control variable settings corresponding to fuel cost-based OPF result in a reduction of 1.13% in fuel cost and significant loss reduction of 44.9%. It can be seen that the results obtained from the PSOGSA are better than those obtained from the above-mentioned methods. This clearly indicates that the proposed PSOGSA can be effectively used to solve the OPF problem for large-scale power systems.

	Initial [29]	PSO	GSA	PSOGSA
Cost ($/hr)	131, 220.52	130, 305.53	129, 873.89	129, 733.58
Ploss (MW)	132.86	80.69	72.31	73.21

TABLE 4. Comparison of the simulation results for IEEE 118-bus test system

5. CONCLUSION

In this article, a hybrid optimization PSOGSA has been proposed and successfully applied to solve the OPF problem. The proposed approach has been tested and investigated on the IEEE 30-bus and the IEEE 118-bus test systems. Simulation results show that the hybrid PSOGSA provides effective and robust high-quality solution. Moreover, the results obtained using the hybrid PSOGSA are either better or comparable to those obtained using other techniques reported in the literature. The proposed hybrid PSOGSA is suitable for solving the complex OPF problem because it benefits from the advantages of both the PSO and GSA.

For practical applications in large-scale power systems, there is need to improve the computational speed; this is the main disadvantage of the PSOGSA.

FUNDING

This work was supported by the Ministry of Education, Science and Technological Development of the Republic of Serbia (research grant TR 33046).

REFERENCES

[1] Abou El Ela, A. A., Abido, M. A., and Spea, S. R., "Optimal power flow using differential evolution algorithm," *Electr. Eng*., Vol. 91, pp. 69–78, 2009.

[2] Frank, S., Steponavice, I., and Rebennack, S., "Optimal power flow: a bibliographic survey I Formulations and deterministic methods," *Energy Syst*., Vol. 3, No. 3, pp. 221–258, 2012.

[3] Frank, S., Steponavice, I., and Rebennack, S., "Optimal power flow: a bibliographic survey II Non-deterministic and hybrid methods," *Energy Syst*., Vol. 3, No. 3, pp. 259–289, 2012.

[4] Ghasemi, M., Ghavidel, S., Rahmani, S., Roosta, A., and Falah, H., "A novel hybrid algorithm of imperialist competitive algorithm and teaching learning algorithm for optimal power flow problem with non-smooth cost function," *Eng. Appl. Art. Intellig.*, Vol. 29, pp. 54–69, 2014.

[5] Narimani, M. R., Azizipanah-Abarghooee, R., Zoghdar-Moghadam-Shahrekohne, B., and Gholami, K., "A novel approach to multi-objective optimal power flow by a new hybrid optimization algorithm considering generator constraints and multi-fuel type," *Energy*, Vol. 49, pp. 119–136, 2013.

[6] Niknam, T., Narimani, M. R., and Azizipanah-Abarghooee, R., "A new hybrid algorithm for optimal power flow considering prohibited zones and valve point effect," *Energy Conv. Manage.*, Vol. 58, pp. 197–206, 2012.

[7] Christy, A. A., and Vimal Raj, P. A. D., "Adaptive biogeography based predator–prey optimization technique for optimal power flow," *Electr. Power Energy Syst*., Vol. 62, pp. 344–352, 2014.

[8] Huang, C. M., and Huang, Y. C., "Hybrid optimisation method for optimal power flow using flexible AC transmission system devices," *IET Gener. Transm. Distrib.*, Vol. 8. No. 12, pp. 2036–2045, 2014.

[9] Alsac, O., and Stott, B., "Optimal load flow with steady-state security," *IEEE Trans. Power App. Syst.*, Vol. 93, No. 3, pp. 745–751, 1974.

[10] Mirjalili, S., and Hashim, S. Z. M., "A new hybrid PSOGSA algorithm for function optimization," *International Conference on Computer and Information Application (ICCIA 2010)*, pp. 374–377, Tianjin, China, 3–5 December 2010.

[11] Mirjalli, S., Hashim, S. Z. M., and Sardroudi, H. M., "Training feedforward neural networks using hybrid particle swarm and gravitational search algorithm," *Appl. Math. Comput*. Vol. 218, pp. 11125–11137, 2012.

[12] Abido, M. A., "Optimal power flow using particle swarm optimization," *Electr. Power Energy Syst.*, Vol. 24, pp. 563–571, 2002.

[13] Rashedi, E., Nezamabadi-pour, H., and Saryazdi, S., "GSA: A gravitational search algorithm," *Inform. Sci.*, Vol. 179, pp. 2232–2248, 2009.

[14] Bouchekara, H. R. E. H., Abido, M. A., and Boucherma, M., "Optimal power flow using teaching–learning-based optimization technique," *Electr. Power Syst. Res*., Vol. 114, pp. 49–59, 2014.

[15] Benasla, L., Belmadani, A., and Rahli, M., "Spiral optimization algorithm for solving combined economic and emission dispatch," *Electr. Power Energy Syst.*, Vol. 62, pp. 163–174, 2014.

[16] Yuryevich, J., and Wong, K. P., "Evolutionary programming based optimal power flow algorithm," *IEEE Trans. Power Syst*., Vol. 14, No. 4, pp. 1245–1250, 1999.

[17] Abdel-Fattah, A., Al-Turki, Y. A, and Abusorrah, A. M., "Optimal power flow using adapted genetic algorithm with adjusting population size," *Electr. Power Compon. Syst*., Vol. 40, pp. 1285–1299, 2012.

[18] Sailaja, K. M., and Maheswarapu, S., "Enhanced genetic algorithm based computation technique for multi-objective optimal power flow," *Electr. Power Energy Syst.*, Vol. 32, pp. 736–742, 2010.

[19] Rezaei, A. M., and Karami, A., "Artificial bee colony algorithm for solving muli-objective optimal power flow problem," *Electr. Power Energy Syst.*, Vol. 53, pp. 219–230, 2013.

[20] Bhattacharya, A., and Chattopadhyay, P. K., "Application of biogeography-based optimisation to solve different optimal power flow problems," *IET Generat. Transm. Distrib.*, Vol. 5, pp. 70–80, 2011.

[21] Basu, M., "Multi-objective optimal power flow with FACTS devices," *Energy Convers. Manag.*, Vol. 52, pp.903–910, 2011.

[22] Ongsakul, W., and Tantimaporn, T., "Optimal power flow by improved evolutionary programming," *Electr. Power Compon. Syst*., Vol. 34, pp. 79–95, 2006.

[23] Duman, S., Guvenc, U., Sonmez, Y., and Yorukeren, N., "Optimal power flow using gravitational search algorithm," *Energy Conv. Manag.*, Vol. 59, pp. 86–95, 2012.

[24] Bakirtzis, A. T., Biskas, P. N., Zoumas, C. E., and Petridis, V., "Optimal power flow by enhanced genetic algorithm," *IEEE Trans. Power Syst.*, Vol. 17, No. 2, pp. 229–236, 2002.

[25] Roy, P. K., and Paul, C., "Optimal power flow using krill herd algorithm," *Int. Trans. Electr. Energ. Syst.*, DOI: 10.1002/etep.1888, 2014.

[26] Lee, K. Y., Park, Y. M., Ortiz, J. L., "A united approach to optimal real and reactive power dispatch," *IEEE Trans. Power App. Syst.*, Vol. 104, No. 5, pp. 1147–1153, 1985.

[27] Abou El Ela, A. A., Abido, M. A., and Spea, S. R., "Optimal power flow using differential evolution algorithm," *Electr. Power Syst. Res*., Vol. 80, pp. 878–885, 2010.

[28] Ghasemi, M., Ghavidel, S., Ghanbarian, M. M., Gharibzadeh, M., and Vahed, A. A., "Multi-objective optimal power flow considering the cost, emission, voltage deviation and power losses using multi-objective modified imperialist competitive algorithm," *Energy*, Vol. 78, pp. 276–289, 2014.

[29] Zimmerman, R. D., Murillo-Sánchez, C. E., *et al.*, "Matpower MATLAB toolbox," 2014, available at: http://www.pserc.cornell.edu//matpower/

BIOGRAPHIES

Jordan Radosavljević received his B.Sc. in 1998 from the Faculty of Electrical Engineering, University of Priština; his M.Sc. in 2003 from the Faculty of Electrical Engineering, University of Belgrade; and his Ph.D. in 2009 from the Faculty of Technical Sciences, University of Priština in Kosovska Mitrovica. Currently, he is an associate professor with the Faculty of Technical Sciences, University of Priština in Kosovska Mitrovica, Serbia. His main research interests include power system analysis and control, power system optimization, and distributed power generation.

Dardan Klimenta received his B.Sc. in 1998 from the Faculty of Electrical Engineering, University of Priština, and his M.Sc. and Ph.D. in 2001 and 2007, respectively, from the Faculty of Electrical Engineering, University of Belgrade. Currently, he is an associate professor with the Faculty of Technical Sciences, University of Priština in Kosovska Mitrovica. His main research interests include application of the finite-element method to power cable field problems, electric power distribution, and distributed power generation.

Miroljub Jevtić received his B.Sc. and M.Sc. in 1980 and 1987, respectively, from the Faculty of Electrical Engineering, University of Skopje; he has a dual Ph.D.—the first in 1989 from the Saint Petersburg State Polytechnic University, Russia and the second in 1991 from the Faculty of Electrical Engineering, University of Skopje, Macedonia. Currently, he is a full professor with the Faculty of Technical Sciences, University of Priština in Kosovska Mitrovica. His main research interests include power cable engineering, electrical insulations, and distributed power generation.

Nebojša Arsić received his B.Sc. in 1983 from the Technical Faculty, University of Priština, and his M.Sc. and Ph.D. in 1989 and 1994, respectively, from the Faculty of Electrical Engineering, University of Belgrade. Currently, he is a full professor with the Faculty of Technical Sciences, University of Priština in Kosovska Mitrovica. His main research interests include high-voltage techniques, high-voltage measurement techniques, modern energy technologies, and materials and renewable energy.